

Potts model on recursive lattices: some new exact results

Pedro D. Alvarez^{1*}, Fabrizio Canfora^{1†}, Sebastián A. Reyes^{2‡}, Simon Riquelme²

¹*Centro de Estudios Científicos (CECS), Valdivia, Chile*

²*Facultad de Física, Pontificia Universidad Católica de Chile, Casilla 306, Santiago 22, Chile*

April 4, 2019

Abstract

By repeated application of the deletion-contraction identity we compute the partition function of the Potts model on lattices with recursive symmetry with arbitrary values of q and temperature parameter $v = e^K - 1$. We first apply the technique to analyze strips of width $L_y = 2$, for three different lattices: square, kagomé and ‘shortest-path’ (to be defined in the text). It is shown that this approach is not restricted to the explicitly solved lattices, but can be applied to a very broad family of graphs of finite width constructed with an arbitrary number of recursive steps. Additionally, we show that the same procedure can be applied to wider strips by solving the kagomé strip of width $L_y = 5$ with the aid of a computer program. As a demonstration of the versatility of the method we construct the exact solution of a recursive lattice similar to strips but whose width changes periodically from $L_y = 3$ to $L_y = m$, where m is an arbitrary integer number. Lastly, we analyze a non-periodic lattice for which the transfer matrix becomes step-dependent.

Keyword: Potts model, exact results, kagomé lattice, diced lattice, dichromatic polynomial.

PACS: 12.40.Nn, 11.55.Jy, 05.20.-y, 05.70.Fh.

1 Introduction

The Potts model [1] is one of the most interesting models in statistical mechanics. It appears as the most natural generalization of the Ising model by allowing the spin variable to take more than two distinct values. Besides its intrinsic importance in the theory of critical phenomena, it manifests a number of intriguing relations with many areas of both physics and mathematics (for nice detailed reviews see [2, 3, 4, 5, 6]; for the relation with the problem of color confinement see [7]; for its relation with the Kohanov Homology see [8]).

We will study the q -state Potts model at zero magnetic field, whose partition function on an arbitrary graph G is,

$$Z(G, q, \beta) = \sum_{\{\sigma_i\}} e^{-\beta \mathcal{H}}$$

where $\beta = 1/k_B T$ and

$$\mathcal{H} = -J \sum_{\langle ij \rangle} \delta_{\sigma_i \sigma_j}.$$

Spin variables σ_i can take values $1, \dots, q$ and are located at the vertices of G . There is also an interaction energy J for pairs of spins located at the ends of every edge $\langle ij \rangle \in G$. It will be important for our development to introduce an equivalent expression for the partition function,

$$Z(G, q, v) = \sum_{\{\sigma_i\}} \prod_{\langle ij \rangle} (1 + v \delta_{\sigma_i \sigma_j}), \quad (1.1)$$

where the temperature variable $v = e^K - 1$ has been introduced with $K \equiv \beta J$. For the ferromagnetic case ($J > 0$) one has $0 \leq v \leq \infty$ corresponding to the temperature interval $\infty \geq T \geq 0$; for the antiferromagnetic Potts ($J < 0$)

*alvarez AT cecs.cl

†canfora AT cecs.cl

‡sreyes AT fis.puc.cl

the interval $-1 \leq v \leq 0$ corresponds to $0 \leq T \leq \infty$. It can be shown directly from (1.1) that the partition function admits also the following polynomial (Fortuin-Kasteleyn) representation [9, 10],

$$Z(G, q, v) = \sum_{G' \subseteq G} q^{k(G')} v^{e(G')} \quad (1.2)$$

where G' is a graph with the same vertex set V of G and an edge set $E' \subseteq E$, with E being the edge set of G ; $k(G')$ and $e(G')$ are respectively the number of connected components and the number of vertices of G' . It is important to notice that using (1.2) one can easily extend q and v from their physical values ($q \in \mathbb{Z}_+$, $v \in [-1, +\infty)$) to the whole complex plane.

Unlike the case of the Ising model ($q = 2$), solved by Onsager [11], the exact solution for the Potts model in any infinite two dimensional lattice is still not available. Nevertheless, thanks to universality, the critical behavior of the ferromagnetic Potts model is fairly well understood. On the other hand, the antiferromagnetic Potts depends on the structural properties of the lattice and its critical properties can vary strongly from case to case. Thus, the search for tools to obtain analytical information on the free energy of the Potts model on generic lattices is a very important task.

An approach that has proven fruitful in recent years is to solve the simpler problem of calculating the partition function for periodic strips of finite width (L_y) and arbitrary length (L_x). Previous work along these lines has relied basically on a transfer matrix method [12, 13, 14, 15, 16] to obtain exact results at arbitrary temperatures for strips of widths going up to $L_y = 7$ (honeycomb lattice with free boundary conditions) [17]. Such efforts have produced detailed studies for the square, triangular, and honeycomb lattices [18, 14, 15, 16, 19, 20, 17, 21].

In many cases it is useful to exploit the recursive structure which is present in lattices of physical interest. Even when the analytic solution is not available, using a simple ansatz which respects the recursive symmetry one can get an excellent agreement with the numerical data [22, 23, 24, 25]. Motivated by these facts we develop a method that permits the calculation of the exact partition function for strips of virtually any kind of lattice.

The idea to use the dichromatic polynomial in the cases of recursive lattices has been proposed in [26, 27, 28], where the authors derive a scalar homogeneous recurrence equation of order higher than one, whose solution is the dichromatic polynomial of the corresponding graph. In the present paper it will be shown that it is possible to extend this idea by formulating vectorial homogeneous order one recurrence equations whose solutions represent the dichromatic polynomials of the graph corresponding to different boundary conditions. As it will be shown in the following sections, this vectorial formulation also allows to deal with recursive lattices which are less regular than strips and whose shapes change with the recursive steps.

The paper is organized as follows: In Sec. 2 we explain the general method and illustrate its use by solving the $L_y = 2$ and $L_y = 3$ square ladders for which the results are already known [13, 16]. Next, in Sec. 3 we present new exact results for arbitrarily long strips of width $L_y = 2$ for the kagomé, diced and ‘shortest path’¹ lattices. In order to demonstrate the versatility of the procedure, in Sec. 5 we obtain the exact solution of a $L_y = 3$ strip corresponding to a mixture of triangular and square lattices, which additionally has periodic attachments of segments of a different strip. Lastly, in Sec. 6 we analyze an interesting case of a non-periodic lattice for which the transfer matrix becomes step-dependent. Conclusions and prospects for future work are discussed in Sec. 7.

2 Recursive equation method

The Potts model partition function on a graph G (Z_G) satisfies the well known deletion-contraction theorem, which says that it can be written in terms of Z_{G_d} and Z_{G_c} as,

$$Z_G = Z_{G_d} + v Z_{G_c}, \quad (2.1)$$

where G_d corresponds to the resulting graph when deleting an arbitrarily chosen edge from G ; and G_c is obtained from G by contracting the same edge (i.e. deleting the edge and identifying the vertices at the end of it). Furthermore, it is easy to show that the Potts model partition function also fulfills the following property,

$$Z_{(\bullet \cup G)} = q Z_G, \quad (2.2)$$

where $Z_{(\bullet \cup G)}$ denotes the partition function of a disjoint union of an isolated vertex and a graph G . The resulting partition function is a polynomial in q and v which in the mathematical literature is known as the dichromatic polynomial of G .

¹This lattice will be introduced in Sec. 3.3. It corresponds to a square lattice plus a graph inside each square that has a topology identical to that of the shortest path joining all four corners.

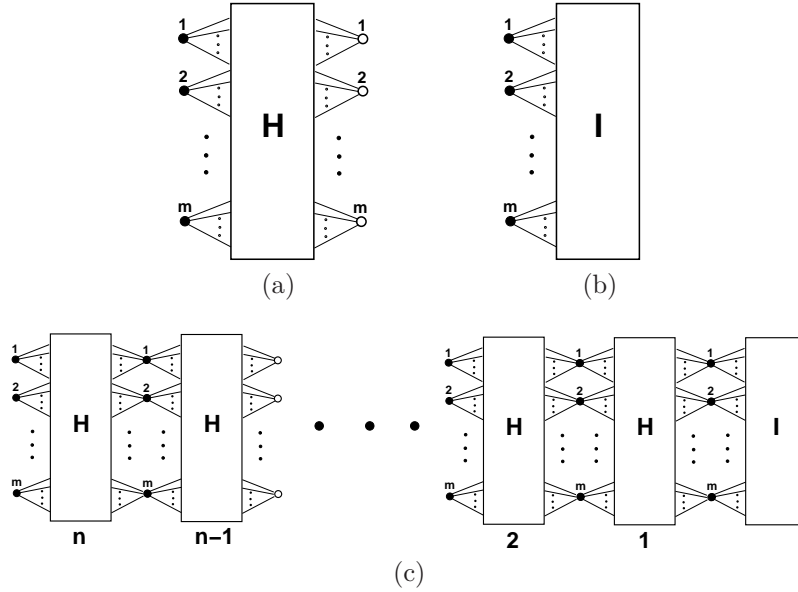


Figure 1: Basic building blocks for a periodic lattice strip. (a) H corresponds to the structure that will be repeated n times. Empty circles to the right denote vertices that will be shared between adjacent blocks. (b) Graph I at the right end of the strip containing the information of the initial condition $\vec{Z}(0) = \vec{Z}_I$. (c) The strip is built up by repeatedly joining H -blocks after I .

Identities (2.1) and (2.2) will form the basis of the method developed in what follows.

Using the notation of [29, 30], consider now strip graphs of the form $(G_s)_n = (\prod_{l=1}^n H)I$, where H is repeatedly attached after the initial subgraph I , which will be put to the right by convention. The junction between contiguous subgraphs is done by sharing a subset of L_y vertices (\tilde{V}) as illustrated in Fig. 1. Each block I or H can contain an arbitrary number of vertices besides the ones in \tilde{V} . Suppose now that starting from a strip of length n as the one shown in Fig. 1c, we apply repeatedly the deletion-contraction theorem to all the edges in the last H block. Once this process is finished, it is easy to see that the partition function of the initial graph ($Z_0(n)$) will be written as a linear combination of the partition functions of objects of length $n - 1$,

$$Z_0(n) = \sum_{j=0}^{N-1} a_{0j}(q, v) Z_j(n-1).$$

The coefficients $a_j(q, v)$ are polynomials in q and v and appear naturally as the edges are contracted (factor v) and vertices become completely disconnected (factor q). A number N of graphs of length $n - 1$ result once all of the edges in the n -th H -block are deleted or contracted. Evidently, these configurations arise from the different ways in which the L_y vertices in \tilde{V} between the n -th and $(n - 1)$ -th H -blocks become identified with each other, by the action of the deletion-contraction theorem over the n -th block. One can proceed analogously starting with each one of the possible $Z_j(n)$; the emerging linear system of equations can be written as

$$\vec{Z}(n) = \mathbf{A}(q, v) \vec{Z}(n-1), \quad (2.3)$$

where $\mathbf{A}(q, v)$ is an N by N matrix with elements $a_{ij}(q, v)$, and the vector $\vec{Z}(n)$ arrange the partition functions for all the various possible connectivities at the top layer. It is worth note that $\mathbf{A}(q, v)$ is independent of the step n : this is a great simplification related to the particular recursive symmetry of the system. As it will be explained in detail below, the dimension N of matrix can be calculated considering only some basic properties of H (i.e. symmetries or if it is planar or not). By recursive use of (2.3), it is straightforward to show that the general solution is

$$\vec{Z}(n) = \mathbf{A}^n(q, v) \vec{Z}(0), \quad (2.4)$$

where $\vec{Z}(0)$ is the partition function vector corresponding to the step-0 block I , in the context of the recursive equations (2.3) $\vec{Z}(0)$ play the roll of initial conditions. We can now use standard linear algebra methods to rewrite

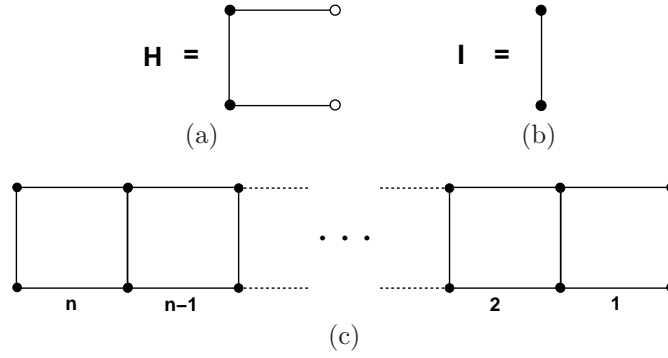


Figure 2: For the square ladder it is quite simple to find its basic building blocks. (a) Every H adds two new vertices (full circles) and three edges. A block is joined to the previous one by sharing the $L_y = 2$ vertices to the left (empty circles). (b) In this case the initial graph I consists of two joined vertices.

the solution (2.4) in the form,

$$\vec{Z}(n) = \sum_{s=0}^{N-1} c_s(q, v) \lambda_s^n(q, v) \vec{\alpha}_s(q, v),$$

where λ_s ($\vec{\alpha}_s$) are the eigenvalues (eigenvectors) of \mathbf{A} , and c_s are some constants sensible to the vector of 0-step lattices $\vec{Z}(0) = \vec{Z}_I$.

Let us now summarize the method by reviewing its basic steps.

Step 1: Identify the periodic structure of the strip and choose basic units (H) which are joined with each other by a set of L_y vertices.

Step 2: Using the deletion-contraction theorem, write down the partition function of a strip of length n as a linear combination of graphs with length $n - 1$. These new graphs will correspond to different ways in which the vertices at the top layer become identified with each other as a result of the deletion-contraction procedure.

Step 3: Repeat Step 2 for all of the possible connectivities at the top layer. The result will be a matrix recurrence equation whose solution in the form (2.4) contains the desired partition function.

This approach has been proposed and applied for zero temperature calculations in [31, 30, 29]. Also, it is important to notice that to find $\mathbf{A}(q, v)$ is equivalent to construct the transfer matrix in the basis of connectivities at the top layer as explained in [14]. Nevertheless, the conventional transfer matrix approach requires a layer by layer construction of horizontal and vertical matrices that strongly restricts the manageable topologies. A clear advantage of the framework presented here, is that it becomes easier to handle complicated lattice topologies, as it will be illustrated below. Lastly, it is worth noticing that the algorithm developed above can be implemented in a computer software in order to handle larger blocks.²

2.1 Application to $L_y = 2$ square ladder

Here we will consider the case of $2 \times n$ square ladder lattices.³ As illustrated in Fig. 2, it is easy to find for this lattice its corresponding initial graph I and its building block H .⁴ For this case we have $L_y = 2$ and by direct calculation it is easy to see that $N = 2$: as explained in Fig. 3, we only have here the original graph corresponding to Z_0 and one graph with the two vertices at the end identified with each other. The vector of the initial graph I is then,

$$\vec{Z}(0) = \begin{pmatrix} q(q+v) \\ q(1+v) \end{pmatrix}. \quad (2.5)$$

In order to construct matrix $\mathbf{A}^{\text{sq}}(q, v)$ for the square (sq) strip, we need to delete and contract all three edges in H as it is explicitly shown and explained in Fig. 4. A similar procedure is followed starting from $Z_1(n)$ to obtain

²In fact, the authors have already developed such a code for $L_y = 2$ systems, in which the user only needs to input the desired graph for the building block H and receives the transfer matrix as an output. Extensions to solve wider strips are obviously possible.

³We solve this system for illustration purposes only since the solution was already obtained in [13].

⁴It is important to observe that there is a certain arbitrariness in the choice of H . For example, one could choose instead to join the graphs by the two vertices along a diagonal of the square.

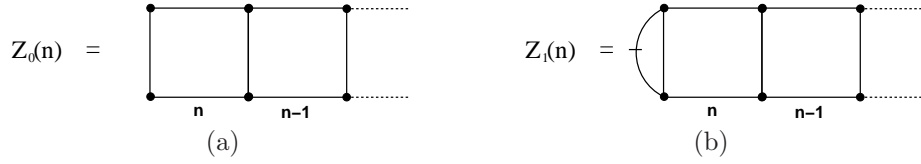


Figure 3: (a) $Z_0(n)$ is the sought partition function which in our convention is the first component of $\vec{Z}(n)$. None of the end vertices of the graph are identified with each other. (b) Once the deletion-contraction theorem is applied to the previous block, a new kind of graph will appear in which the two leftmost vertices are identified with each other. In our notation identified vertices are joined by a crossed line.

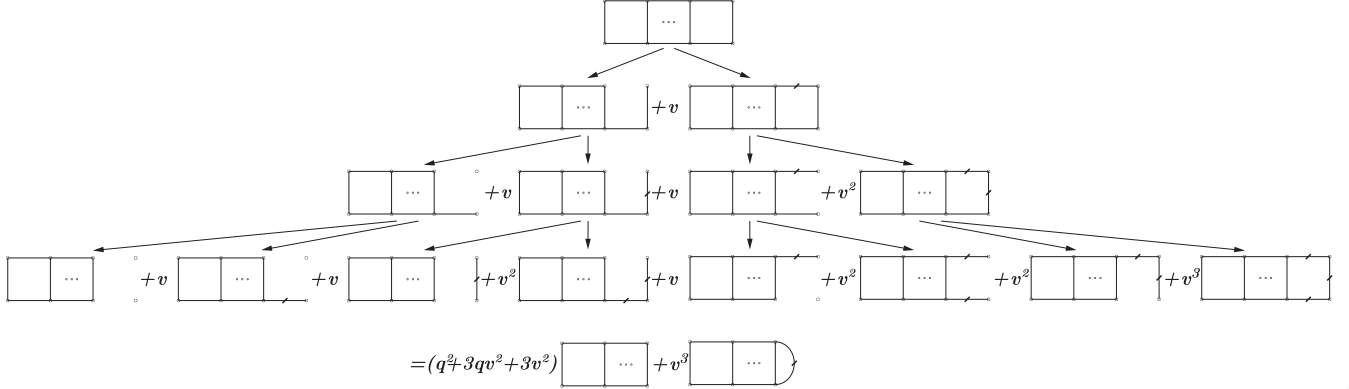


Figure 4: The deletion-contraction theorem (2.1) is applied successively to each edge in the last block. As a result, the partition function of the original graph of length n is written as a linear combination of the partition functions of two distinctive objects of length $n - 1$.

finally,

$$\mathbf{A}^{\text{sq}}(q, v) = \begin{pmatrix} (q + v)(q + 2v) + v^2 & v^3 \\ (1 + v)(q + 2v) & (1 + v)v^2 \end{pmatrix}.$$

It is now trivial to diagonalize this 2×2 matrix to find that its eigenvalues are

$$\lambda_{\pm}^{\text{sq}}(q, v) = \frac{1}{2}(q^2 + 3qv + 4v^2 + v^3 \pm \sqrt{q^4 + 6q^3v + 13q^2v^2 + 16qv^3 - 2q^2v^3 + 12v^4 - 2qv^4 + 4v^5 + v^6}). \quad (2.6)$$

As it is well known, the dominant eigenvalue λ_+ will determine the free energy in the thermodynamic limit. It can be noted that the discriminant is always positive in the physical regime.

2.2 Solution of the $L_y = 3$ square lattice

In order to illustrate how our method can be also used for lattices with $L_y > 2$ we solve here explicitly the $3 \times n$ square lattice. The exact solution for such a system was first derived in [16].

The idea, as before, is to use rules (2.1) and (2.2) to derive a relation between the partition functions of the lattices of length n and $n - 1$:

$$\vec{Z}_{(3)}^{\text{sq}}(n) = \mathbf{A}_{(3)}^{\text{sq}}(q, v) \vec{Z}_{(3)}^{\text{sq}}(n - 1), \quad (2.7)$$

where,

$$\mathbf{A}_{(3)}^{\text{sq}}(q, v) = \begin{pmatrix} a_{11} & a_{12} & a_{13} & a_{14} \\ a_{21} & a_{22} & a_{23} & a_{24} \\ a_{31} & a_{32} & a_{33} & a_{34} \\ a_{41} & a_{42} & a_{43} & a_{44} \end{pmatrix}.$$

The four components of $\vec{Z}_{(3)}^{\text{sq}}$ are the partition functions on a $3 \times n$ square ladder lattice in which on the rightmost vertices the four basic identification have been respectively performed (see Fig. 5). As in the previous subsection, the functions a_{ij} are easily computed using the rules (2.1) and (2.2). The exact values of the functions a_{ij} are indicated in Table 1.

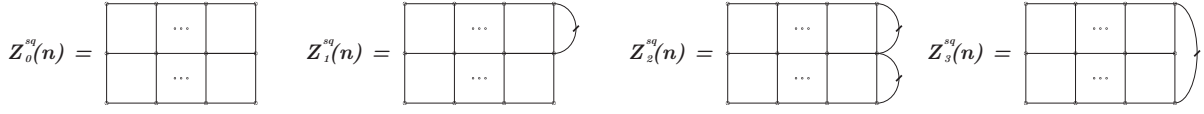


Figure 5: The four components of the partition function vector correspond to the different ways the vertices at the end of the lattice can be identified with each other as a result of the deletion contraction procedure.

$$\begin{aligned}
a_{11} &= (q + 2v)(q^2 + 3qv + 4v^2), & a_{12} &= 2v^3(q + 2v), & a_{13} &= v^5, & a_{14} &= v^4, \\
a_{21} &= (1 + v)(q^2 + 4qv + 5v^2), & a_{22} &= v^2(1 + v)(q + 3v), & a_{23} &= v^4(1 + v), & a_{24} &= v^3(1 + v), \\
a_{31} &= (q + 3v)(1 + v)^2, & a_{32} &= 2v^2(1 + v)^2, & a_{33} &= v^3(1 + v)^2, & a_{34} &= v^2(1 + v)^2, \\
a_{41} &= q^2 + 5qv + 8v^2 + qv^2 + 3v^3, & a_{42} &= 2v^3(2 + v), & a_{43} &= v^4(2 + v), & a_{44} &= v^2(q + 3v + v^2).
\end{aligned}$$

Table 1: Values of the functions a_{ij} .

One can easily obtain the initial condition by building the vector $\vec{Z}_{(3)}^{\text{sq}}(0)$ of the partition functions of the elementary 3×1 ladders shown in Fig. 6,

$$\vec{Z}_{(3)}^{\text{sq}}(0) = \begin{pmatrix} q(q + v)^2 \\ q(q + v)(1 + v) \\ q(1 + v)^2 \\ q(q + 2v + v^2) \end{pmatrix}. \quad (2.8)$$

The resulting partition function for any n is then:

$$\vec{Z}_{(3)}^{\text{sq}}(n) = \left[\mathbf{A}_{(3)}^{\text{sq}} \right]^n \vec{Z}_{(3)}^{\text{sq}}(0)$$

Thus, the present method provides one with results which are equivalent to the ones obtained with more usual methods [16].

3 Some new exact results for $L_y = 2$ strips

In order to illustrate the power of the method described above, we will use it now to obtain the exact partition function for strips of three different lattices: kagomé, diced and ‘shortest-path’ (described below). To analyze the results we plot for each case the internal energy per site and specific heat as a function of the temperature variable v , for different values of q .

Internal energy and specific heat are quantities that can be obtained straightforwardly from the free energy by taking the appropriate derivatives as follows:

$$E = -\frac{\partial f}{\partial \beta} = -J(v + 1) \frac{\partial f}{\partial v} \quad (3.1)$$

and

$$\frac{C}{k_B} = \frac{1}{k_B} \frac{\partial E}{\partial T} = K^2(v + 1) \left[\frac{\partial f}{\partial v} + (v + 1) \frac{\partial^2 f}{\partial v^2} \right]. \quad (3.2)$$

In the limit of infinite length the free energy per site becomes

$$f = \frac{1}{N_{uc}} \ln \lambda_d, \quad (3.3)$$

where N_{uc} is the number of sites per unit cell and λ_d is the dominant eigenvalue of the transfer matrix. For simplicity, instead of the internal energy, we will plot the dimensionless quantity $-E/J$, which has the virtue of having the same sign for both the ferromagnetic ($0 \leq v \leq \infty$) and antiferromagnetic ($-1 \leq v \leq 0$) physical regions.

3.1 Kagomé lattice strip

The kagomé lattice is the medial graph of both the triangular and hexagonal lattices. The Potts model on this network is a prototypical highly frustrated system and has been widely studied for many years. Nevertheless, in

$$Z_0^{sq}(0) = \begin{array}{c} | \\ | \\ | \end{array} \quad Z_1^{sq}(0) = \begin{array}{c} \curvearrowright \\ | \\ | \end{array} \quad Z_2^{sq}(0) = \begin{array}{c} \curvearrowright \\ \curvearrowright \\ | \end{array} \quad Z_3^{sq}(0) = \begin{array}{c} \curvearrowright \\ \curvearrowright \\ \curvearrowright \end{array}$$

Figure 6: These partitions functions of these four graphs constitute the initial condition vector $\vec{Z}_{(3)}^{sq}(0)$.

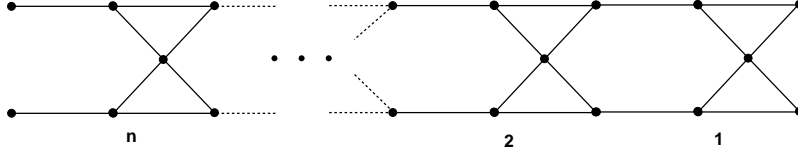


Figure 7: A strip of the kagomé lattice with $L_y = 2$. Each unit cell is composed of five vertices and eight edges. The transfer matrix for this unit cell (eq. (3.4)) is obtained by successive application of the deletion-contraction theorem.

contrast with simpler lattices like the square, triangular or honeycomb [32, 33, 34], many fundamental questions such as the exact determination of the critical frontier remain unresolved in the kagomé network [35, 36, 37, 38]. In this context, exact results for kagomé strips of finite width may provide some insight into the properties of the model in two dimensions.

We proceed to use our recursive equation method to calculate the exact partition function for the $L_y = 2$ kagomé strip shown in Fig. 7. The resulting transfer matrix is,

$$\mathbf{A}^k(q, v) = \begin{pmatrix} a_{11}^k & a_{12}^k \\ a_{21}^k & a_{22}^k \end{pmatrix}, \quad (3.4)$$

where,

$$a_{11}^k = q^5 + 8q^4v + 28q^3v^2 + 54q^2v^3 + 2q^3v^3 + 59qv^4 + 10q^2v^4 + 30v^5 + 20qv^5 + 16v^6 + qv^6 + 2v^7, \quad (3.5)$$

$$a_{12}^k = q^2v^4 + 6qv^5 + 9v^6 + 2qv^6 + 6v^7 + v^8, \quad (3.6)$$

$$a_{21}^k = q^4 + 8q^3v + 27q^2v^2 + q^3v^2 + 46qv^3 + 10q^2v^3 + 36v^4 + 30qv^4 + 2q^2v^4 \quad (3.7)$$

$$+ 34v^5 + 10qv^5 + 14v^6 + qv^6 + 2v^7, \quad (3.8)$$

$$a_{22}^k = 2qv^4 + 12v^5 + 13v^6 + 6v^7 + v^8. \quad (3.9)$$

It is now straightforward to obtain the eigenvalues of this two by two matrix. They will not be written here explicitly but, as explained above, they are used to calculate the internal energy and specific heat that are displayed in Fig. 8.

Due to frustration, a finite zero-temperature internal energy is observed for $q = 2$ in the antiferromagnetic regime ($v = -1$). It is actually not hard to find the exact ground state configuration which consists of only two edges per unit cell with energy $-J$. Since there are five sites per unit cell, the energy per site becomes $-2J/5 = -0.4J$ as observed in Fig. 8a. For larger values of q there is no frustration and the energy goes to zero as $v \rightarrow -1$. At low temperatures on the ferromagnetic side ($v \rightarrow \infty$) the ground state consists always in an alignment of all the spins. Thus, each one of the eight edges in the unit cell will have energy $-J$, resulting in an energy per site of $-8J/5 = -1.6J$, as shown in Fig. 8a.

The specific heat presents a peak in the ferromagnetic side, which is related to the phase transition known to be present in the 2D kagomé lattice. As the strip widens, the peak will evolve into a characteristic discontinuity of the transition. Furthermore, since the Wu conjecture [35] determines with great accuracy that the ferromagnetic critical points are located at $v_c(q = 2) \approx 1.542$, $v_c(q = 3) \approx 1.876$ and $v_c(q = 4) \approx 2.156$, we know that the position of the peaks will move to the left for wider strips.

As expected, the Potts antiferromagnet is much more complicated. The $q = 2$ case on the kagomé lattice has been solved exactly [39] and it is known to present no phase transition at any temperature. Moreover, it is expected that the $q = 3$ model is critical at zero temperature [40, 41] and that it remains noncritical for any $q > 3$. Thus, the peaks for $v < 0$ observed in Fig. 8b are not expected to evolve into phase transition divergences as the strip widens for $q = 2, 4$; whereas for $q = 3$ we do expect that to be the case. It is interesting to note that indeed the most pronounced maxima corresponds to $q = 3$.

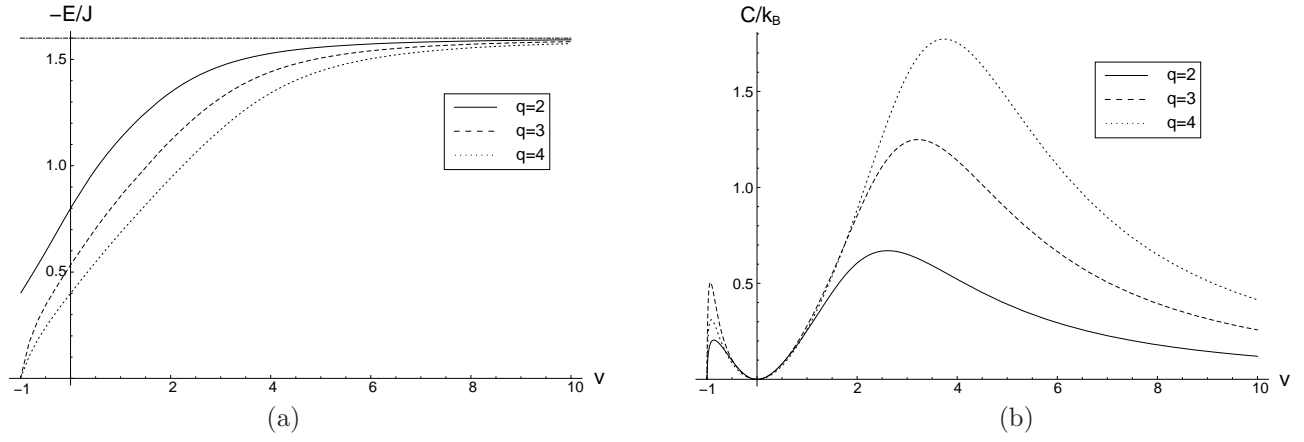


Figure 8: Results for the kagomé lattice strip. (a) Reduced internal energy as a function of the temperature parameter $v = e^K - 1$ for different values of q . Lattice frustration gives rise to a finite zero-temperature internal energy for $q = 2$. (b) Dimensionless specific heat as a function of v .

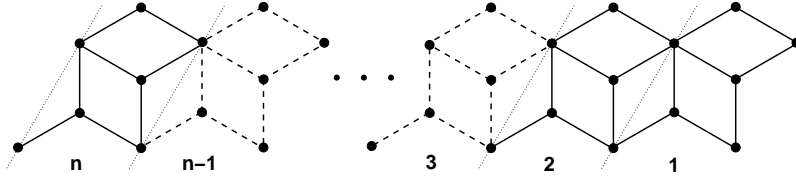


Figure 9: A strip of the diced lattice with $L_y = 2$. Each unit cell is composed of five vertices and eight edges. A dashed line marks the division between unit cells.

3.2 Diced lattice strip

The diced lattice consists on a periodic tiling of the plane by rhombi and is the dual of the kagomé lattice. The Potts model on the two-dimensional diced lattice has interesting critical properties. For instance, it has been shown recently [42] that, even though it admits a height mapping representation for $q = 3$, it contradicts theoretical expectations having $q_c(\text{diced}) > 3$. Furthermore, it is the first known case of a two-dimensional bipartite lattice with $q_c > 3$.

We calculate here the exact partition function for the $L_y = 2$ diced lattice strip shown in Fig. 9. Proceeding as before, applying the deletion-contraction theorem to all the vertices in a block, the elements of the resulting two by two transfer matrix $\mathbf{A}^d(q, v)$ are,

$$a_{11}^d = q^5 + 8q^4v + 27q^3v^2 + 50q^2v^3 + 52qv^4 + 2q^2v^4 + 26v^5 + 7qv^5 + 9v^6 + v^7, \quad (3.10)$$

$$a_{12}^d = q^4v^2 + 6q^3v^3 + 16q^2v^4 + 22qv^5 + q^2v^5 + 15v^6 + 4qv^6 + 7v^7 + v^8, \quad (3.11)$$

$$a_{21}^d = q^4 + 8q^3v + 26q^2v^2 + q^3v^2 + 44qv^3 + 6q^2v^3 + 33v^4 + 19qv^4 + 26v^5 + 2qv^5 + 8v^6 + v^7, \quad (3.12)$$

$$a_{22}^d = q^3v^2 + 6q^2v^3 + 17qv^4 + q^2v^4 + 20v^5 + 8qv^5 + 19v^6 + qv^6 + 7v^7 + v^8. \quad (3.13)$$

By the method described above we can now compute the internal energy and specific heat (see Fig. (10)).

In this case there is no frustration and even for $q = 2$ we observe that the energy reaches $E = 0$ at zero temperature. On the ferromagnetic side, the spins become aligned at zero temperature and the minimal value of energy per site $E = -8J/5$, is reached.

For $q = 2$ the model has been solved exactly in two dimensions and it is known to present an antiferromagnetic transition at $v \approx -0.3401$ [39]. Thus, we expect that the observed peak in the specific heat will evolve into the corresponding divergence for infinite width. On the other hand, since for $q = 3$ and 4 the lattice is known to have no antiferromagnetic phase transition, we expect that for such values of q the specific heat peaks at $v < 0$ will disappear or move below $v = -1$ as the strip widens.

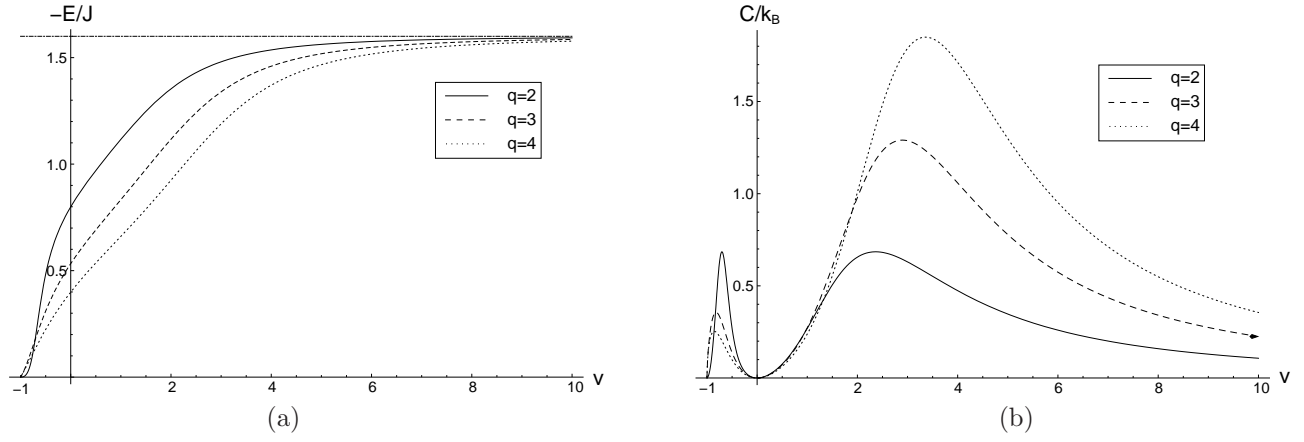


Figure 10: Results for the diced lattice strip. (a) Reduced internal energy as a function of the temperature parameter $v = e^K - 1$ for different values of q . (b) Dimensionless specific heat as a function of v .

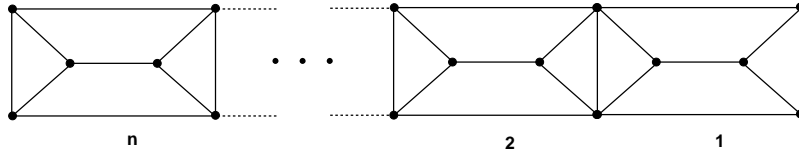


Figure 11: A strip of the “shortest path” lattice with $L_y = 2$. Each unit cell is composed of four vertices and eight edges.

3.3 “Shortest-path” lattice strip

Here we will consider the case of a lattice strip which we will call “shortest path”, since its topology naturally appears when one solves the problem of the shortest path connecting the vertices of a square (see Fig. 11). The recursive equation method yields the following result for the elements of the transfer matrix $\mathbf{A}^{\text{sh}}(q, v)$,

$$a_{11}^{\text{sh}} = q^4 + 8q^3v + 27q^2v^2 + 48qv^3 + q^2v^3 + 40v^4 + 7qv^4 + 16v^5 + 2v^6, \quad (3.14)$$

$$a_{12}^{\text{sh}} = q^3v^2 + 7q^2v^3 + 23qv^4 + 35v^5 + 5qv^5 + 26v^6 + 8v^7 + v^8, \quad (3.15)$$

$$a_{21}^{\text{sh}} = q^3 + 7q^2v + q^3v + 18qv^2 + 8q^2v^2 + 20v^3 + 23qv^3 + q^2v^3 + 32v^4 + 5qv^4 + 14v^5 + 2v^6, \quad (3.16)$$

$$a_{22}^{\text{sh}} = 2q^2v^2 + 10qv^3 + 2q^2v^3 + 20v^4 + 13qv^4 + 39v^5 + 3qv^5 + 26v^6 + 8v^7 + v^8. \quad (3.17)$$

Internal energy and specific heat are plotted in Fig. 12 for different values of q .

Frustration for $q = 2$ is manifested in the finite energy at zero temperature in the antiferromagnetic side. As for the case of the kagomé strip, it is easy to find the minimum energy configuration for this system and find that its energy becomes $E = -J/4$, as can be verified in Fig. 12(a).

Although to our knowledge this lattice has not been studied before, due to universality in the ferromagnetic side it is safe to state that the observed specific heat maxima at $v > 0$ are related to the divergences at the transitions expected in two dimensions. On the other hand, the Potts antiferromagnet is highly dependent on its lattice structure and extracting information about its critical properties would require further study.

As a further illustration of the power of the present method, in Appendix A we briefly analyze the Fisher zeros for the square and the “shortest-path” lattices in the standard range of values of q and also in the large q limit.

4 Kagomé strip $L_y = 5$

In previous sections we have demonstrated the versatility of the deletion-contraction procedure in handling basically any lattice strip of width $L_y = 2$. We will now show that the method can also be applied to wider strips. So far, the calculations have been simple enough so that they can be managed by hand. Nevertheless, as the strips become wider, the size of the transfer matrices grows rapidly and performing the corresponding calculations requires the

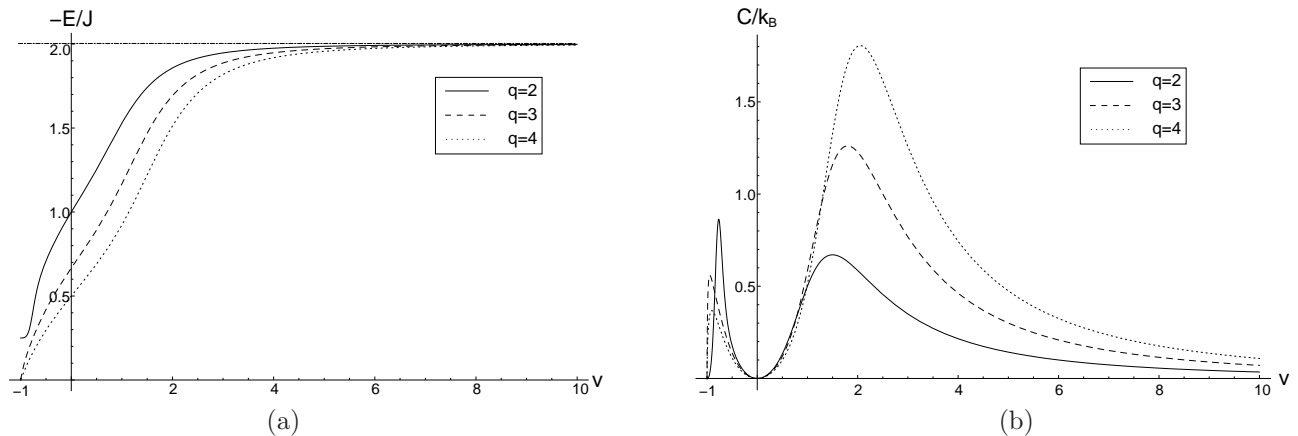


Figure 12: Results for the “shortest path” lattice strip. (a) Reduced internal energy as a function of the temperature parameter $v = e^K - 1$ for different values of q . (b) Dimensionless specific heat as a function of v .

assistance of a computer software. In particular, the size of the transfer matrix for a kagomé strip of *odd* width L_y under free boundary conditions is given by Catalan’s number,

$$C_{L_y} = \frac{1}{L_y + 1} \binom{2L_y}{L_y}, \quad (4.1)$$

which gives the number of non-crossing partitions of the set $\{1, 2, \dots, L_y\}$.⁵ Thus, for a kagomé strip of width $L_y = 5$ we need to calculate a 42×42 transfer matrix.

To achieve this we have developed a code in *Mathematica* that is able to handle such a convoluted calculation. Basically, the code performs the same task that one would do by hand: Repeatedly apply the deletion contraction theorem to one block of the strip. It does so for each one of the 42 possible initial graphs and by keeping track of the coefficients corresponding to the final graphs, it constructs the desired transfer matrix. The result is obviously too lengthy to display here, but is available upon request from the authors.

As before, the specific heat can be calculated using (3.2). The result displayed in Fig. 13, shows some interesting features. In the ferromagnetic side the maxima become more pronounced as expected for wider strips. Furthermore, all of the peaks come closer to the phase transition points expected for the two dimensional kagomé lattice ($v_c(q = 2) \approx 1.542$, $v_c(q = 3) \approx 1.876$ and $v_c(q = 4) \approx 2.156$).

5 Ornamented $L_y = 3$ hybrid strip

So far we have dealt with topologically complicated but otherwise regular strips. However, within the same framework, we can solve even more complex periodic structures such as the configuration depicted in Fig. 14. It consists of a mixture of square and triangular strips decorated by segments of the shortest-path lattice. Obviously, one expects that for such a lattice the construction of the exact solution should become much more difficult. There are two main reasons for this: Firstly, in this example the lattice has not one but three different types of basic boxes (square, triangular and shortest path in the above example). Thus, the system has less symmetries and the dimension of the corresponding transfer matrix increases. Secondly, the shape is not regular so that it is not obvious how to apply the more usual techniques in this case. Nevertheless, such cases can still be efficiently handled within our framework.

To understand how can one deal with this complicated lattice it is convenient to think of the problem in different steps. First, we decompose the ornament of the last block making use of the corresponding transfer matrix calculated in this case in Sec. 3.3. It is easy to notice that at the end of this process we end up with the two types of blocks shown in Fig. 14(b). Following again the method described in Sec. 2, we can then calculate their corresponding 5×5 transfer matrices $A^{(1)}$ and $A^{(2)}$ that enable us to decompose the main body of the strip. Lastly, by combining these steps we obtain,

$$\vec{Z}(n) = \left(\alpha(m)A^{(1)} + \beta(m)A^{(2)} \right) A^{(1)} \vec{Z}(n-1), \quad (5.1)$$

⁵For *even* widths L_y the size is reduced due to reflection symmetry.

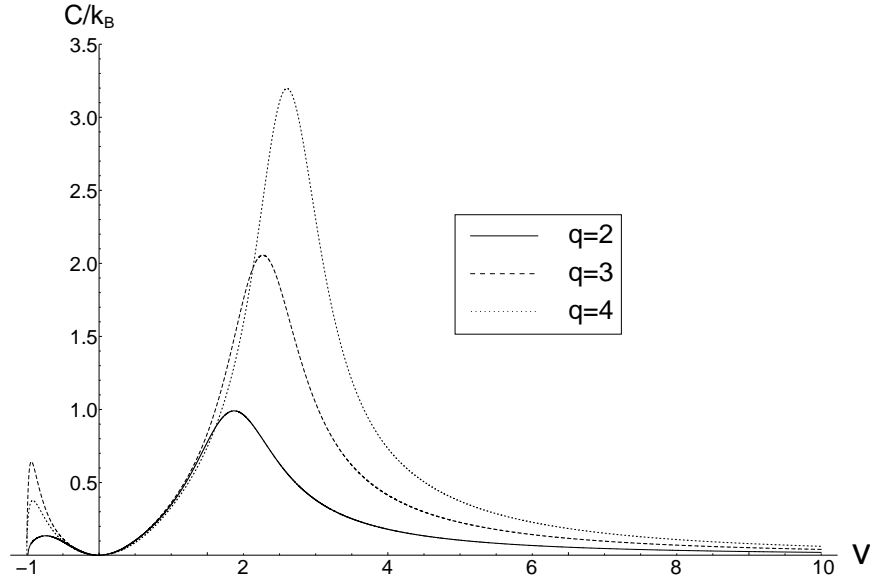


Figure 13: Specific heat for an infinite kagomé lattice strip of width $L_y = 5$ as a function of v .

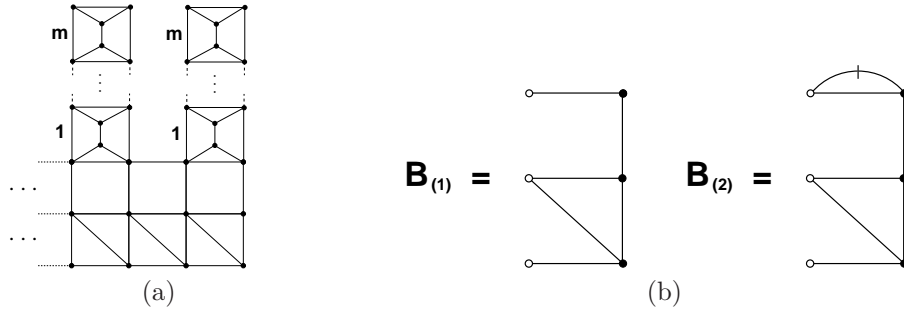


Figure 14: (a) Right end of a mixture of triangular and square lattices “ornamented” periodically by a series of shortest-path strips of length m . (b) Intermediate blocks $B_{(1)}$ and $B_{(2)}$ to be considered in the calculation of the full transfer matrix of the structure in (a).

where $\alpha(m)$ and $\beta(m)$ are scalar quantities given by

$$\alpha(m) = \left\{ \left(\mathbf{A}^{\text{sh}}(q, v) \right)^m \right\}_{1,1}, \quad \beta(m) = \left\{ \left(\mathbf{A}^{\text{sh}}(q, v) \right)^m \right\}_{1,2}. \quad (5.2)$$

The details of the calculation and explicit expressions for all of the matrices involved can be found in the Appendix. Using the same method as in previous cases, we can extract the internal energy and specific heat displayed in Fig. 15.

Finally, we point out that the solution outlined here can be straightforwardly generalized for any type of $L_y = 2$ ornament for which the transfer matrix is known. One only needs to replace $\alpha(m)$ and $\beta(m)$ accordingly in (5.1).

6 Step-dependent transfer matrix

In previous sections, it has been shown how to exploit directly the periodic recursive symmetry of lattices. The idea so far has been to derive a homogeneous first order linear recurrence relation for a vector which allows to solve recursive lattices which are more general than strip lattices. The reason is that our vectorial recursive system of equations only need periodic recursive symmetry in order to be applied. Therefore, one can also analyze ornamented strip lattices which are, as it has been already explained, strip lattices whose geometry and width can change periodically. To achieve this goal, it is very important to analyze *all the components* of our vectorial recursive system of equations, and not just the component which represents the sought partition function. It is

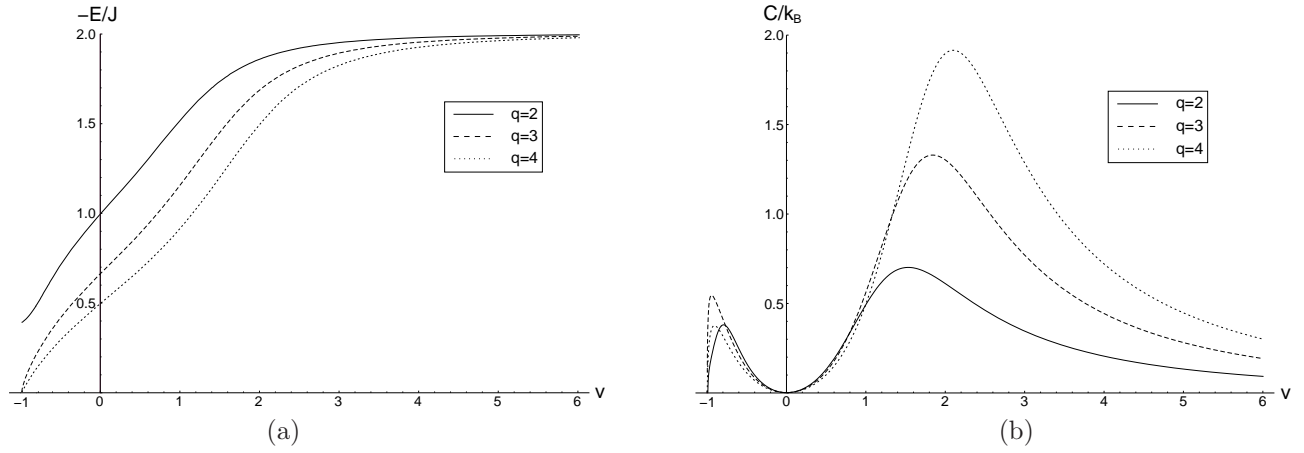


Figure 15: Results for the “ornamented” lattice strip in Fig. 14a. (a) Reduced internal energy as a function of the temperature parameter $v = e^K - 1$ for different values of q . (b) Dimensionless specific heat as a function of v .

the interplay between the different components of the vector which provides one with the possibility to build up the exact solutions of ornamented strip lattices. In this sense, the present formalism is an extension of the classic results of Biggs, et. al. [26] and of Beraha, et. al. [27, 28] in which the authors considered a homogeneous higher order linear recurrence relation with “constant coefficients”⁶ for a scalar in order to find the partition function of periodic strip lattices.

In this section, we will present a system which is quite interesting since it discloses a possibility to further extend these results. Up to now, we have only analyzed cases in which the lattice has a periodic recursive symmetry, namely the recursive steps to construct the lattice are “always the same” as in the cases of strip lattices as well as ornamented strip lattices. Indeed, these are the most analyzed cases in the literature. On the other hand, the key idea of the present method also works for recursive non-periodic lattices. We will now show how to apply the present formalism to these cases as well.

An interesting example is the lattice depicted in the Fig. 16. The resulting linear system will indeed have an n -dependent transfer matrix,

$$\vec{Z}(n) = A(n)\vec{Z}(n-1) \quad (6.1)$$

with,

$$A(n) = \begin{pmatrix} \frac{1}{q}(T(n+2) - qv^{n+2}) & v^{n+2} \\ \frac{q+2v}{q}T(n) & \frac{v^2}{q}T(n) \end{pmatrix}, \quad (6.2)$$

where $T(n)$ stands for the partition function of the ring with n vertices given by

$$T(n) = qv^n + q \sum_{i=0}^{n-1} v^i (q+v)^{n-1-i}. \quad (6.3)$$

The n -dependence in (6.2) is a manifestation of the fact that each new layer in the lattice is not the same as the previous one. Nevertheless, it is possible to apply the method in exactly the same way as before. The vector of the partition function can be written in the form

$$\vec{Z}(n) = A(n)A(n-1)\dots A(1)\vec{Z}(0), \quad (6.4)$$

where the boundary term is given by the two component vector $\vec{Z}(0) = (q, q)$. The partition function can be read from the first component of (6.4). Moreover, it turns to be quite complicated to resolve in general the characteristic equation corresponding to the recursive equation of the present example because the coefficients depends on n .

7 Conclusions and perspectives

We have exploited a method based on the deletion-contraction theorem to obtain a variety of new exact results for the partition function of the Potts model. It has been demonstrated that this technique is quite effective even in

⁶Namely, a linear recurrence relation whose coefficients do not depend explicitly on the recursive step n .

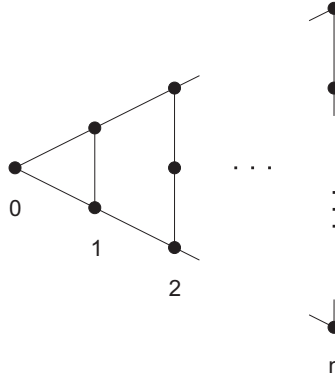


Figure 16: Example of a lattice in which the transfer matrix of every layer explicitly depends on the recursive step n .

many cases in which the lattice topology is complicated. Indeed, in order for such a method to be applied, the only requirement is that the lattice has a recursive symmetry while there is no need to assume extra symmetries.

In the case of lattice strips, we have shown that the technique is *not* restricted to be applied to the simpler cases of $L_y = 2$ or 3 . With the aid of a computer program we were able to find the exact transfer matrix for the $L_y = 5$ kagomé strip. In future work we intend to use the same approach to obtain exact results for the $L_y = 5$ dimered lattice strip.

It has also been shown that this procedure can be easily applied to recursive lattices similar to strips but whose width changes periodically (for instance, from $L_y = 3$ to $L_y = m$, where m is an arbitrary integer number). The possibility to analyze lattices with less regular shapes than strips is a great advantage of the present method and could be quite important for applications.

It is worth noting that this technique can be extended to deal with other boundary conditions such as periodic, toroidal or Möbius. Wider strips, which may capture two dimensional features more faithfully, can be considered as well. Furthermore, since the calculation procedure is purely combinatoric, it works equally well for non-planar graphs. This approach offers also new perspectives for the analysis of scaling and the large q limit.

Appendix A: Some remarks on Fisher zeros and the large- q limit

It is sometimes useful to find the zeros of the partition function in the complex v plane. These are the so called Fisher zeros which have been used to develop very powerful tools in statistical mechanics [43, 44, 45, 46, 47, 48]. We will show the Fisher zeros of the square and “shortest-path” strip lattices for two ranges of values of q : small integers and the large q limit.

When q is in the small integer range the structure of the Fisher zeros for the two lattices is very sensible to the topology of the lattice as illustrated in Fig. 17. On the other hand, when q is very large it is worth noting that the curve in the complex plane simplifies to a circle (see Fig. 18).

Let us now consider the recursive lattice studied in Sec. 6. The n -dependent transfer matrix depends explicitly on $T(n)$ which is the partition function of a ring made of n segments. Therefore, it is natural to expect that the specific heat of this lattice will present many peaks corresponding to the various factors $T(n')$ ($n' = 1, \dots, n$) appearing in the exact expression of the partition function. This expectation is confirmed in Fig. 19, where the large- q specific heat displays these features.

Appendix B: Ornamented strip transfer matrix

As explained in the main text, one can proceed by first decomposing the ornament and then the main body of the strip. Combining both of these procedures the resulting transfer matrix is given by,

$$\vec{Z}(n) = \left(\alpha(m)A^{(1)} + \beta(m)A^{(2)} \right) A^{(1)} \vec{Z}(n-1), \quad (7.1)$$

where $\alpha(m)$ and $\beta(m)$ are scalar quantities that can be extracted directly from the transfer matrix of the “ornamented” strip,

$$\alpha(m) = \left\{ \left(\mathbf{A}^{\text{sh}}(q, v) \right)^{m-1} \right\}_{1,1}, \quad \beta(m) = \left\{ \left(\mathbf{A}^{\text{sh}}(q, v) \right)^{m-1} \right\}_{1,2}. \quad (7.2)$$

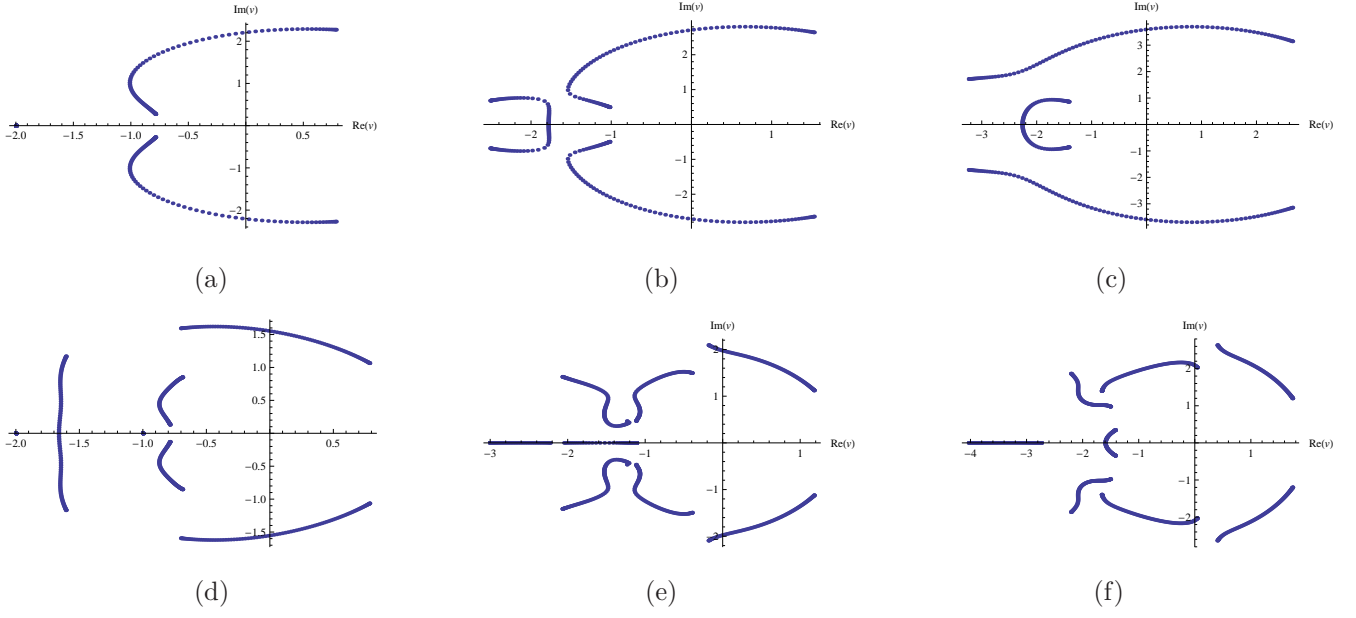


Figure 17: The Fisher zeros are plotted in the complex v plane for strips of length $n = 100$ for the square lattice in the cases (a) $q = 2$ (b) $q = 3$ and (c) $q = 5$; and for the “shortest-path” in cases (d) $q = 2$, (e) $q = 3$ and (f) $q = 5$.

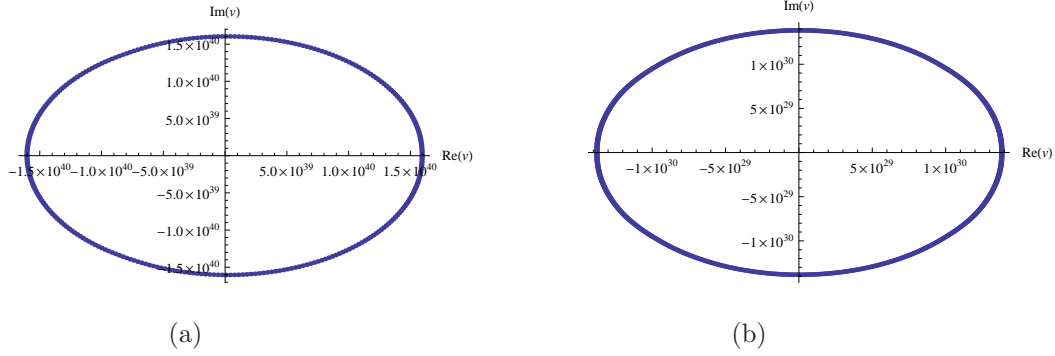


Figure 18: The Fisher zeros are plotted for strips of length $n = 100$ and $q = 2^{200}$ for: (a) square lattice and (b) “shortest-path” lattice.

On the other hand, $A^{(1)}$ and $A^{(2)}$ are 5×5 matrices given by

$$A^{(1)} = \begin{pmatrix} B_{s_1, s_2}^{c_1, c_2, c_3} & C_{s_2}^{c_1, c_3} & D_{s_1, s_2}^{c_2, c_4, c_5} & E_{s_2}^{c_2, c_4, c_5} & F_{s_2}^{c_2} \\ B_{t_1, t_2}^{c_1, c_2, c_3} & C_{t_2}^{c_1, c_3} & D_{t_1, t_2}^{c_2, c_4, c_5} & E_{t_2}^{c_2, c_4, c_5} & F_{t_2}^{c_2} \\ B_{s_1, s_2}^{d_1, d_2, d_3} & C_{s_2}^{d_1, d_3} & D_{s_1, s_2}^{d_2, d_4, d_5} & E_{s_2}^{d_2, d_4, d_5} & F_{s_2}^{d_2} \\ B_{t_1, t_2}^{d_1, d_2, d_3} & C_{t_2}^{d_1, d_3} & D_{t_1, t_2}^{d_2, d_4, d_5} & E_{t_2}^{d_2, d_4, d_5} & F_{t_2}^{d_2} \\ \tilde{B}_{c_1, c_2, c_3; d_1, d_2, d_3}^{e_1, e_2, e_3, e_4} & \tilde{C}_{e_3, e_4} & \tilde{D}_{c_2, c_4, c_5; d_2, d_4, d_5}^{e_1, e_2} & \tilde{E}_{e_3, e_4} & \tilde{F}_{e_3, e_4} \end{pmatrix}, \quad (7.3)$$

$$A^{(2)} = (1 + v) \begin{pmatrix} B_{s_3, s_4}^{c_1, c_2, c_3} & C_{s_4}^{c_1, c_3} & D_{s_3, s_4}^{c_2, c_4, c_5} & E_{s_4}^{c_2, c_4, c_5} & F_{s_4}^{c_2} \\ B_{t_3, t_4}^{c_1, c_2, c_3} & C_{t_4}^{c_1, c_3} & D_{t_3, t_4}^{c_2, c_4, c_5} & E_{t_4}^{c_2, c_4, c_5} & F_{t_4}^{c_2} \\ B_{s_3, s_4}^{d_1, d_2, d_3} & C_{s_4}^{d_1, d_3} & D_{s_3, s_4}^{d_2, d_4, d_5} & E_{s_4}^{d_2, d_4, d_5} & F_{s_4}^{d_2} \\ B_{t_3, t_4}^{d_1, d_2, d_3} & C_{t_4}^{d_1, d_3} & D_{t_3, t_4}^{d_2, d_4, d_5} & E_{t_4}^{d_2, d_4, d_5} & F_{t_4}^{d_2} \\ \tilde{B}_{c_1, c_2, c_3, d_1, d_2, d_3}^{f_1, f_2, f_3, f_4} & \tilde{C}_{f_3, f_4} & \tilde{D}_{c_2, c_4, c_5, d_2, d_4, d_5}^{f_1, f_2} & \tilde{E}_{f_3, f_4} & \tilde{F}_{f_3, f_4} \end{pmatrix}, \quad (7.4)$$

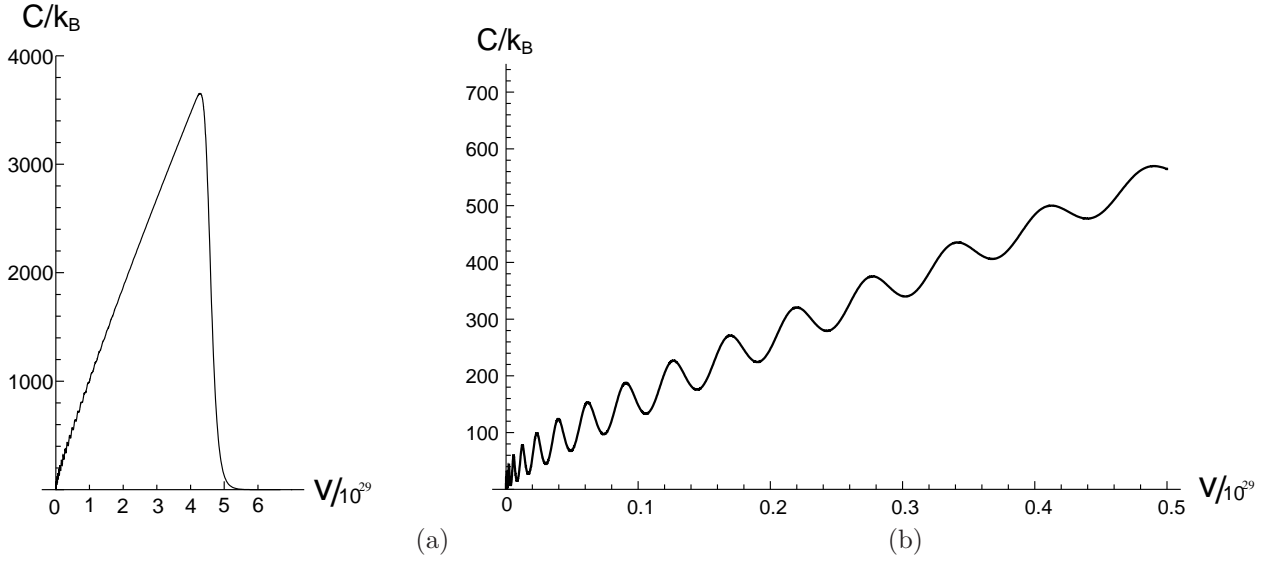


Figure 19: (a) Specific heat in the ferromagnetic range for the $n = 50$ lattice. A global maximum and many local peaks in the high temperature regime are observed. (b) Lower temperature regime in more detail. The density of local peaks is observed to increase with temperature.

where,

$$B_{s_1, s_2}^{c_1, c_2, c_3} = s_1((q+v)c_1 + c_2 + (1+v)c_3) + s_2c_1, \quad (7.5)$$

$$C_{s_2}^{c_1, c_3} = s_2(vc_1 + (1+v)c_3), \quad (7.6)$$

$$D_{s_1, s_2}^{c_2, c_4, c_5} = s_1(vc_2 + (q+v)c_4 + (1+v)c_5) + s_2c_4, \quad (7.7)$$

$$E_{s_2}^{c_2, c_4, c_5} = s_2(vc_2 + vc_4 + (1+v)c_5), \quad (7.8)$$

$$F_{s_2}^{c_2} = s_2c_2, \quad (7.9)$$

$$\begin{aligned} \tilde{B}_{c_1, c_2, c_3, d_1, d_2, d_3}^{e_1, e_2, e_3, e_4} &= e_1((q+v)c_1 + c_2 + (1+v)c_3) + e_2((q+v)d_1 + d_2 + (1+v)d_3) \\ &\quad + (q+2v)e_3 + (1+v)e_4, \end{aligned} \quad (7.10)$$

$$\tilde{C}_{e_3, e_4} = v(v + T_2/q)e_3 + v(1+v)(2+v)e_4, \quad (7.11)$$

$$\tilde{D}_{c_2, c_4, c_5, d_2, d_4, d_5}^{e_1, e_2} = e_1(vc_2 + (q+v)c_4 + (1+v)c_5) + e_2(vd_2 + (q+v)d_4 + (1+v)d_5), \quad (7.12)$$

$$\tilde{E}_{e_3, e_4} = v^2(v + T_2/q)e_3 + v^2(1+v)(2+v)e_4, \quad (7.13)$$

$$\tilde{F}_{e_3, e_4} = v(q+2v)e_3 + v(1+v)e_4, \quad (7.14)$$

$$(7.15)$$

with $T_2 = q(q+2v) + qv^2$, and

$$s_1 = q+2v, \quad s_2 = v^2, \quad s_3 = 1, \quad s_4 = v, \quad (7.16)$$

$$t_1 = 1+v, \quad t_2 = v(1+v), \quad t_3 = 0, \quad t_4 = 1+v, \quad (7.17)$$

$$c_1 = q+3v, \quad c_2 = v^2, \quad c_3 = v^2, \quad c_4 = v^2, \quad c_5 = v^3, \quad (7.18)$$

$$d_1 = (1+v), \quad d_2 = v(1+v), \quad d_3 = v(1+v), \quad d_4 = 0, \quad d_5 = v^2(1+v), \quad (7.19)$$

$$e_1 = 1, \quad e_2 = v, \quad e_3 = v, \quad e_4 = v^2, \quad (7.20)$$

$$f_1 = 0, \quad f_2 = 0, \quad f_3 = 1, \quad f_4 = v. \quad (7.21)$$

$$(7.22)$$

As usual the general expression for the vector of partition functions is given by

$$\vec{Z}(n) = \left[\left(\alpha(m)A^{(1)} + \beta(m)A^{(2)} \right) A^{(1)} \right]^{n-1} \vec{Z}(1), \quad (7.23)$$

where the initial data correspond to the vector

$$\vec{Z}(1) = \begin{pmatrix} q(q+v)^2 \\ q(q+v)(1+v) \\ q(q+v)(1+v) \\ q(1+v)^2 \\ q(q+v) + qv(1+v) \end{pmatrix} \quad (7.24)$$

Acknowledgements

The authors want to give a very warm thank for his illuminating comments and suggestions to Marco Astorino who participated to the early stage of this project. S. A. R. wishes to thank Rafael Benguria for kind support and many fruitful discussions. This work was supported by Fondecyt grants 11080056, 3100140. S. A. R. acknowledges financial support from VRAID (PUC) and Facultad de Física (PUC). The Centro de Estudios Científicos (CECS) is funded by the Chilean Government through the Millennium Science Initiative and the Centers of Excellence Base Financing Program of Conicyt and Conicyt grant "Southern Theoretical Physics Laboratory" ACT-91. CECS is also supported by a group of private companies which at present includes Antofagasta Minerals, Arauco, Empresas CMPC, Indura, Naviera Ultragás and Telefónica del Sur.

References

- [1] Potts, R. B. (1952) *Proc. Cambridge Philos. Soc.* **48**, 106.
- [2] Wu, F. Y. (1982) *Reviews of Modern Physics* **54(1)**, 235.
- [3] Baxter, R. J. (2008) *Exactly Solved Models in Statistical Mechanics*, Dover Publications, .
- [4] Wu, F. Y. (1992) *Rev. Mod. Phys.* **64(4)**, 1099–1131.
- [5] Yang, C. N. and Ge, M. L. (1994) *Braid group, knot theory and statistical mechanics II*, World Scientific, .
- [6] Cardy, J. *Conformal invariance and percolation* (2001).
- [7] Svetitsky, B. and Yaffe, L. G. (1982) *Nuclear Physics B* **210(4)**, 423–447.
- [8] Kauffman, L. H. (2009) *ArXiv e-prints (0907.3178v2)*.
- [9] Fortuin, C. M. and Kasteleyn, P. W. (1972) *Physica* **57**, 536.
- [10] Kasteleyn, P. W. and Fortuin, C. M. (1969) *J. Phys. Soc. Japan* **26(Suppl.)**, 11.
- [11] Onsager, L. (1944) *Phys. Rev.* **65(3-4)**, 117–149.
- [12] Blöte, H. W. J. and Nightingale, M. P. (1982) *Physica A: Statistical and Theoretical Physics* **112(3)**, 405.
- [13] Shrock, R. (2000) *Physica A: Statistical Mechanics and its Applications* **283(3-4)**, 388–446.
- [14] Salas, J. and Sokal, A. D. (2001) *Journal of Statistical Physics* **104(3/4)**, 609.
- [15] Jacobsen, J. L. and Salas, J. (2001) *Journal of Statistical Physics* **104(3/4)**, 701.
- [16] Chang, S.-C., Salas, J., and Shrock, R. (2002) *Journal of Statistical Physics* **107(5/6)**, 1207.
- [17] Chang, S.-C. (2008) *Journal of Statistical Physics* **130(5)**, 1011.
- [18] Chang, S.-C. and Shrock, R. (2001) *Physica A: Statistical Mechanics and its Applications* **296(1-2)**, 234–288.
- [19] Chang, S.-C. and Shrock, R. (2004) *Journal of Statistical Physics* **114(3/4)**, 763.
- [20] Chang, S.-C. and Shrock, R. (2001) *Physica A: Statistical Mechanics and its Applications* **296(1-2)**, 183–233.
- [21] Salas, J. and Sokal, A. D. (2009) *Journal of Statistical Physics* **135(2)**, 279.
- [22] Canfora, F. (2007) *Physics Letters B* **646(1)**, 54–61.

- [23] Astorino, M., Canfora, F., Martínez, C., and Parisi, L. (2008) *Physics Letters B* **664**(1-2), 139–144.
- [24] Astorino, M., Canfora, F., and Giribet, G. (2009) *Physics Letters B* **671**(2), 291–297.
- [25] Astorino, M. and Canfora, F. (2010) *Accepted for publication in Phys. Rev. E (arXiv:0901.2711)*.
- [26] Biggs, N. L., Damerell, R. M., and Sands, D. A. (1972) *J. Combin. Theory* **B12**, 123–131.
- [27] Beraha, S. and Kahane, J. (1979) *J. Combin. Theory* **B27**, 1–12.
- [28] Beraha, S., Kahane, J., and Weiss, N. J. (1980) *J. Combin. Theory* **B28**, 56–65.
- [29] Rocek, M., Shrock, R., and Tsai, S.-H. (1998) *Physica A Statistical and Theoretical Physics* **252**(3-4), 505.
- [30] Rocek, M., Shrock, R., and Tsai, S.-H. (1998) *Physica A Statistical and Theoretical Physics* **259**(3-4), 367.
- [31] Shrock, R. and Tsai, S.-H. (1998) *Physica A: Statistical and Theoretical Physics* **259**(3-4), 315–348.
- [32] Baxter, R. J. (1973) *Journal of Physics C: Solid State Physics* **6**(23), L445.
- [33] Baxter, R. J., Temperley, H. N. V., and Ashley, S. E. (1978) *Proceedings of the Royal Society of London. Series A, Mathematical and Physical Sciences (1934-1990)* **358**(1695), 535.
- [34] Hintermann, A., Kunz, H., and Wu, F. Y. (1978) *Journal of Statistical Physics* **19**(6), 623.
- [35] Wu, F. Y. (1979) *Journal of Physics C: Solid State Physics* **12**(17), L645.
- [36] Hu, C.-K., Chen, J.-A., and Wu, F. Y. (1994) *Modern Physics Letters B [Condensed Matter Physics; Statistical Physics and Applied Physics]* **8**(7), 455.
- [37] Chen, J.-A., Hu, C.-K., and Wu, F. Y. (1999) *Journal of Physics A: Mathematical and General* **31**(39), 7855.
- [38] Monroe, J. L. (2003) *Phys. Rev. E* **67**(1), 017103.
- [39] Syozi, I. (1972) In C. Domb and M. S. Green, (ed.), *Phase Transitions and Critical Phenomena*, Vol. 1, : Academic Press, New York.
- [40] Huse, D. A. and Rutenberg, A. D. Apr 1992 *Phys. Rev. B* **45**(13), 7536–7539.
- [41] Kondev, J. and Henley, C. L. (1996) *Nuclear Physics B* **464**(3), 540.
- [42] Kotecký, R., Salas, J., and Sokal, A. D. (2008) *Physical Review Letters* **101**(3), 030601.
- [43] Yang, C. N. and Lee, T. D. Aug 1952 *Phys. Rev.* **87**(3), 404–409.
- [44] Lee, T. D. and Yang, C. N. Aug 1952 *Phys. Rev.* **87**(3), 410–419.
- [45] Abe, R. (1967) *Progress of Theoretical Physics* **37**(6), 1070–1079.
- [46] Abe, R. (1967) *Progress of Theoretical Physics* **38**(1), 72–80.
- [47] Suzuki, M. (1967) *Progress of Theoretical Physics* **38**(1), 289–290.
- [48] Suzuki, M. (1968) *Progress of Theoretical Physics* **39**(2), 349–364.